

## 4. Linear Modulation Schemes

In these schemes, the amplitude of the modulated signal varies linearly with the modulating digital signal  $m(t) = m_i \cdot g_{T_b}(t)$ , where  $g(\cdot)$  is the chosen pulse shape and  $T_b$  is the pulse duration.

- Transmitted signal is given by

$$s(t) = \Re[A \cdot m(t) \cdot e^{j2\pi f_c t}] = A \cdot [m_R(t) \cos(2\pi f_c t) - m_I(t) \sin(2\pi f_c t)] \quad (4.1)$$

where  $A$  is the amplitude,  $f_c$  is the carrier frequency, and  $m(t) = m_R(t) + jm_I(t)$  is a complex envelope representation of the modulated signal.

- While linear modulation schemes have a very good spectral efficiency, they must be transmitted using linear transmitter amplifier, which have poor power efficiency.
- Using non-linear power efficient amplifiers leads to sidelobes in signal, which can cause adjacent channel interference (very critical for emerging highly multiplexed communication systems!). Some efficient techniques exist to circumvent that, which includes QPSK,  $\pi/4$ PSK and a number of similar techniques.

### 4.1 Binary Phase Shift Keying (BPSK)

Phase of a constant amplitude carrier signal is switched between two values according to message symbols  $m_i$ . If the sinusoidal carrier (simple modifications needed for other carrier signals) has an amplitude  $A_c$ , a pulse duration  $T_b$  and energy-per-bit  $E_b = A_c^2 T_b / 2$ , then the transmitted signal is given by:

$$S_{BPSK}(t) = \sqrt{\frac{2E_b}{T_b}} \begin{cases} \cdot \cos(2\pi f_c t + \mathbf{q}_c) & \text{if } 0 \leq t \leq T_b \text{ for binary "1"} \\ \cos(2\pi f_c t + \mathbf{p} + \mathbf{q}_c) & \text{if } 0 \leq t \leq T_b \text{ for binary "0"} \end{cases} \quad (4.2)$$

If we represent the message as:  $m(t) = \{m_0, m_1\}$ , we can rewrite (3.18):

$$S_{BPSK}(t) = m(t) \cdot \sqrt{\frac{2E_b}{T_b}} \cos(2\pi f_c t + \mathbf{q}_c) = \Re[g_{BPSK}(t) \cdot e^{j2\pi f_c t}] \quad (4.3)$$

where the complex envelop form of BPSK is defined by:

$$g_{BPSK}(t) = m(t) \cdot \sqrt{\frac{2E_b}{T_b}} \cdot e^{j\mathbf{q}_c} \quad (4.4)$$

Note that the last exponential term due to initial phase shift can be dropped without any loss of generality if  $\mathbf{q}_c = 0$ .

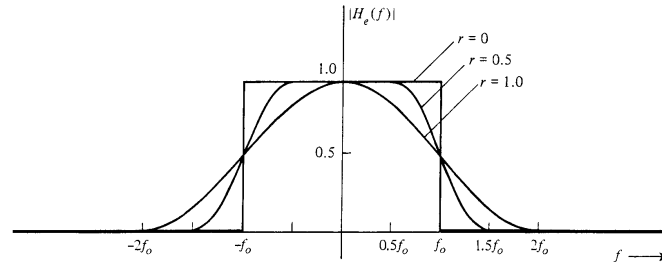
- **Power Spectral Density** of the envelope of BPSK signal is given by:

$$P_{g\_BPSK}(f) = 2 \cdot E_b \cdot \left( \frac{\sin \pi f T_b}{\pi f T_b} \right)^2 \quad (4.5)$$

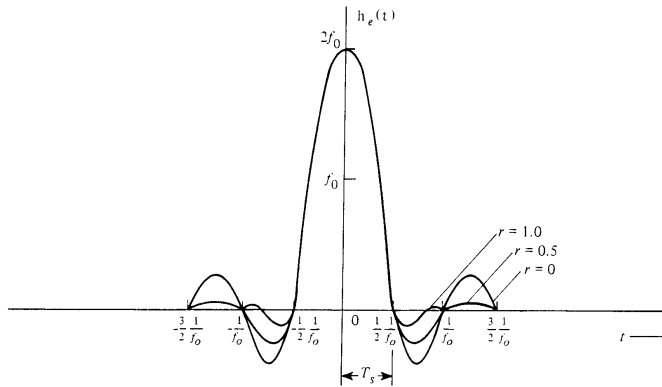
and the PSD of the modulated BPSK is given by:

$$P_{BPSK}(f) = \frac{E_b}{2} \left[ \left( \frac{\sin \pi (f - f_c) T_b}{\pi (f - f_c) T_b} \right)^2 + \left( \frac{\sin \pi (-f - f_c) T_b}{\pi (-f - f_c) T_b} \right)^2 \right] \quad (4.6)$$

Sidelobes of this spectrum as plotted below can be drastically reduced if the pulse shape is replaced with the family of Raised-Cosine Roll-off Pulse shapes.



(a) Magnitude Frequency Response



(b) Impulse Response

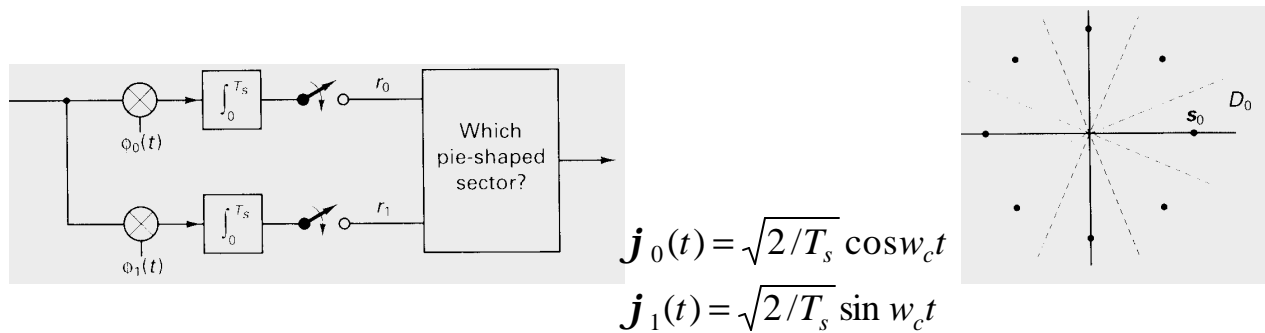
**Note 1:** The null-to-null BW is equal to twice the bit rate:

$$BW = 2R_b = 2/T_b \quad (4.7)$$

**Note 2:** It is observed from these curves that 90% of the BPSK signal energy is contained within a bandwidth approximately equal to  $1.6R_b$  for rectangular pulse and all of the energy is within  $1.5R_b$  for pulses with  $a = 0.5$  raised-cosine filtered pulse.

**Optimal BPSK Receiver Performance:**

If we present the architecture for a generic M-PSK receiver and then the BPSK and other derived cases can be easily configured.

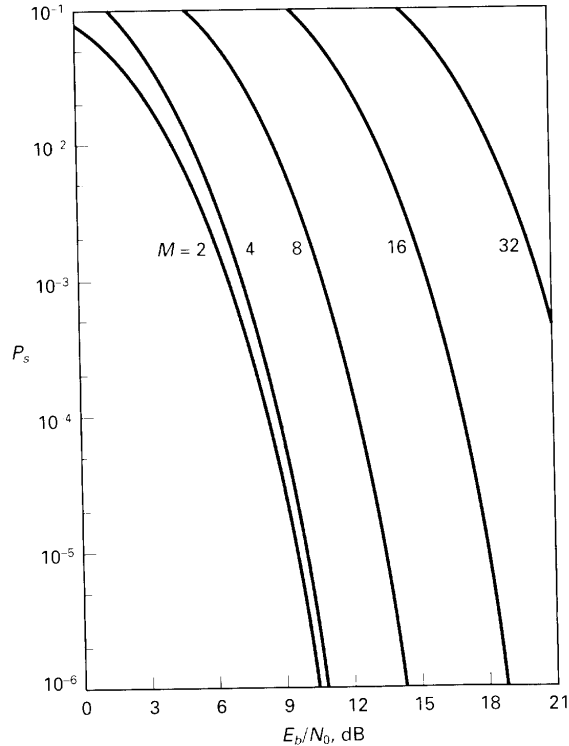


From the signal-space symmetry, the probability of correct decision given that  $S_i(t)$  was the transmitted signal, is independent of the index  $i$  and

$$P(C | m_0) = 1 - P_s = r \int_0^\infty \frac{\exp[-\frac{(r_0 - m)^2}{2s^2}] r_0 \cdot \tan(\pi/M) \exp[-\frac{r_1^2}{2s^2}]}{(2ps^2)^{1/2}} \left[ \int_0^{\tan(\pi/M)} \frac{1}{(2ps^2)^{1/2}} \right] dr_0 \quad (4.8)$$

Hopelessly unfriendly expression! But for  $M=2$ , this expression collapses to the "antipodal binary"

signaling with a BER:  $P_s = Q\left(\sqrt{\frac{2E_b}{N_0}}\right)$ . Numerical integration of (4.8) is shown below.



**Note 1:** Every doubling of  $M$ , the distance between points on a circle is approximately halved. Thus, doubling of  $M$  projects a 6.0 dB loss in energy efficiency when  $M$  is large as it can be observed from the above curves.

**Note 2:** It has been shown in the literature that the energy efficiency, relative to antipodal signaling, is given by:

$$h_{MPSK} = (\log_2 M) \cdot \sin^2(\pi/M) \quad (4.9)$$

which drops by roughly 6 dB for every doubling of  $M$ , when  $M$  is large.

- Bit error probability (BER) is bit assignment dependent since it effects the nearest-neighbor errors.
- To improve that Gray-coded labeling is recommended. We present the Gray-coded labeling for 4-PSK (QPSK) and 8-PSK cases.
- Furthermore, BER for QPSK is exactly the same as that of binary PSK when they are compared at equal  $E_b/N_0$ . This is expected since in Gray coding each information bit is resolved in a binary test of one half-plane against another.
- The distance to the decision boundary is  $\sqrt{E_s/s} = \sqrt{E_b}$  thus yielding:

$$BER = P_b = Q\left(\sqrt{2E_b/N_0}\right) \quad \text{Gray-Coded QPSK} \quad (4.10)$$

**Note 3:** Despite this equivalence in energy efficiency with BPSK, QPSK signals occupy only half the spectrum that BPSK occupies for a given bit rate, producing one of those rare occurrences of something for almost nothing! Consequently, QPSK has become the base-line technique for many modern communication systems. Price to pay is the increased sensitivity to carrier phase synchronization error. However, with PLL and Costa's Loop type measures this is not a major hurdle.

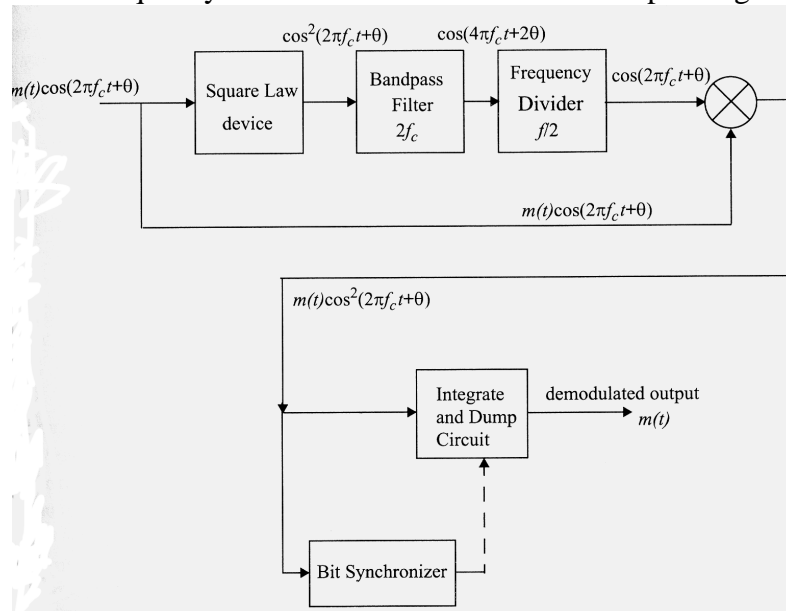
### BPSK Receivers

In the case, no multipath impairments are induced by the channel, the received BPSK signal is

$$S_{BPSK}(t) = m(t) \cdot \sqrt{\frac{2E_b}{T_b}} \cos(2\pi f_c t + \mathbf{q}_c + \mathbf{q}_{ch}) \quad (4.11)$$

where  $\mathbf{q}_{ch}$  is the phase shift corresponding the time-delay in the channel.

- Due to phase nature, the BPSK receivers are coherent or synchronous demodulators, in which the carrier phase and the frequency are extracted from the low-level pilot signal using a PLL.



- The multiplier output after the frequency divider is simply:

$$m(t) \sqrt{\frac{2E_b}{T_b}} \cdot \cos^2(2\pi f_c t + \mathbf{q}_c + \mathbf{q}_{ch}) = m(t) \sqrt{\frac{2E_b}{T_b}} \left[ \frac{1}{2} + \frac{1}{2} \cos 2(2\pi f_c t + \mathbf{q}) \right] \quad (4.12)$$

where  $\mathbf{q} = \mathbf{q}_c + \mathbf{q}_{ch}$

- Integrate-dump circuit forms the LP segment of the signal. If the transmitter and the receiver pulse shapes are matched then the detector output will be optimum. The sampled output at the end of each bit period is compared to a threshold to decide whether it is "1" or "0."

### 4.2 Differential PSK (DPSK)

DPSK is a non-coherent form of PSK avoiding the need for a coherent reference signal at the receiver. Thus, a reduced cost in implementation. Differentially encoded sequence  $\{d_k\}$  is

generated from the input binary message sequence  $\{m_k\}$  by complimenting the modulo-2 operation:

$$d_k = \overline{m_k \oplus d_{k-1}} \quad (4.13)$$

A BPSK to Binary DPSK translation table is given below.

$m_k$		1	0	0	1	0	1	1	0
$d_{k-1}$		1	1	0	1	1	0	0	0
$d_k$	1	1	0	1	1	0	0	0	1

The transmitter and receiver block diagrams are simple extensions of BPSK.

While DPSK has the advantage of reduced receiver complexity, its energy efficiency is inferior to that of coherent PSK by about 3 dB.

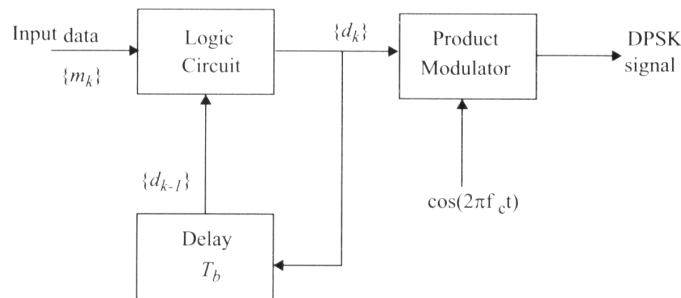


Figure 5.24  
Block diagram of a DPSK transmitter.

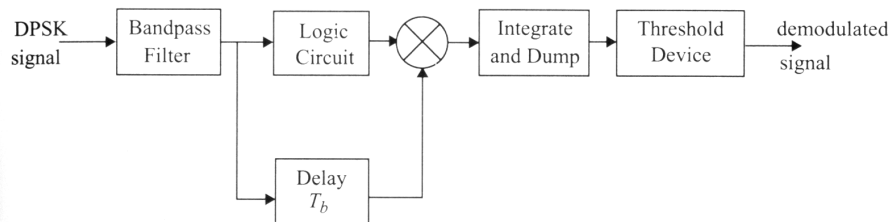


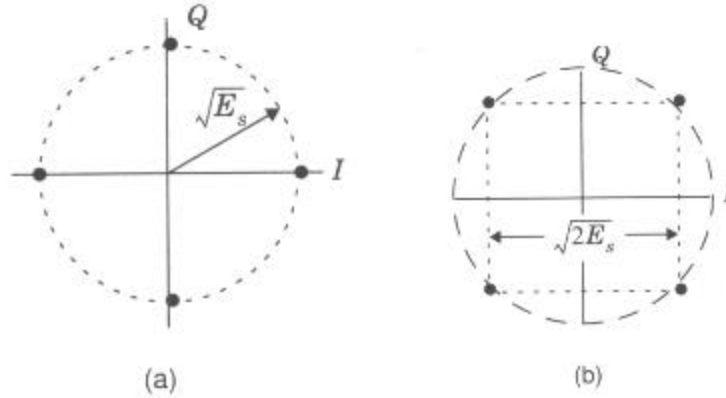
Figure 5.25  
Block diagram of DPSK receiver.

The average BER for DPSK under AWGN is given by:

$$P_{DPSK}(\mathbf{e}) = \frac{1}{2} \cdot e^{-\frac{E_b}{N_0}} \quad (4.14)$$

### 4.3 Quadrature Phase Shift Keying (QPSK)

It has twice the bandwidth efficiency of BPSK as mentioned above. The phase of the carrier takes on 1 of 4 equally spaced values as shown below.



QPSK constellation with phases  $\{0, \mathbf{p}/2, \mathbf{p}, 3\mathbf{p}/2\}$  and their 45 degrees shifted version.

The QPSK signal for the first constellation above is simply:

$$S_{QPSK}(t) = \sqrt{\frac{2E_s}{T_s}} \cdot \text{Cos}(2\mathbf{p}f_c t + (i-1)\frac{\mathbf{p}}{2}) \quad \text{for } 0 \leq t \leq T_s \text{ and } i=1,2,3,4 \quad (4.15)$$

where the symbol duration:  $T_s = 2.T_b$ , the bit period. From the constellation diagram we see that the distance between adjacent samples is  $\sqrt{2E_s}$  and since each symbol corresponds to 2-bits then  $E_s = 2.E_b$ . The distance in QPSK then becomes  $2\sqrt{E_b}$ . Substituting the above into the generic probability equation we obtain the BER for QPSK:

$$BER_{QPSK} = P_{QPSK}(\mathbf{e}) = Q(\sqrt{2E_b}/N_0) \quad (4.16)$$

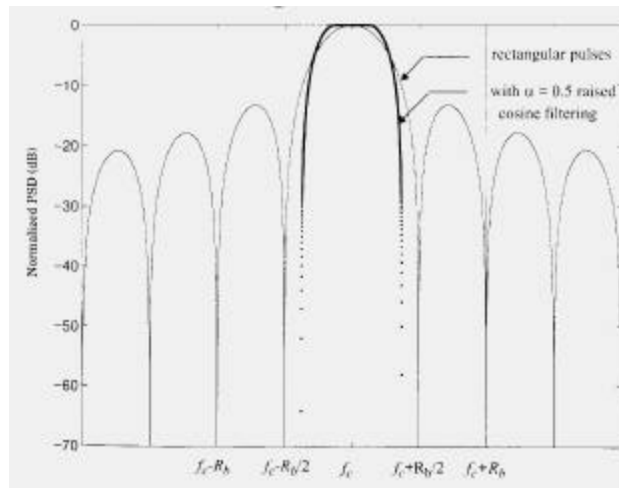
QPSK can be differentially encoded as in the case of DSPK to allow non-coherent detection.

### PSD and Bandwidth of QPSK:

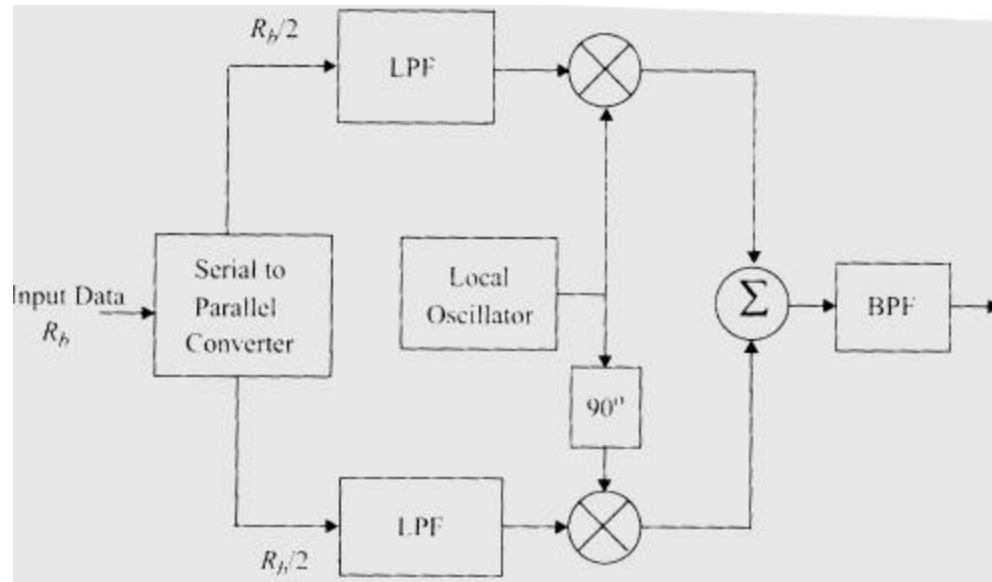
PSD in this case for rectangular pulses will be similar to PSK where symbol duration  $T_s$  has to replace the bit period  $T_b$ :

$$P_{QPSK}(f) = \frac{E_s}{2} \cdot \left[ \left( \frac{\text{Sin} \mathbf{p} T_s (f - f_c)}{\mathbf{p} T_s (f - f_c)} \right)^2 + \left( \frac{\text{Sin} \mathbf{p} T_s (-f - f_c)}{\mathbf{p} T_s (-f - f_c)} \right)^2 \right] \quad (4.17)$$

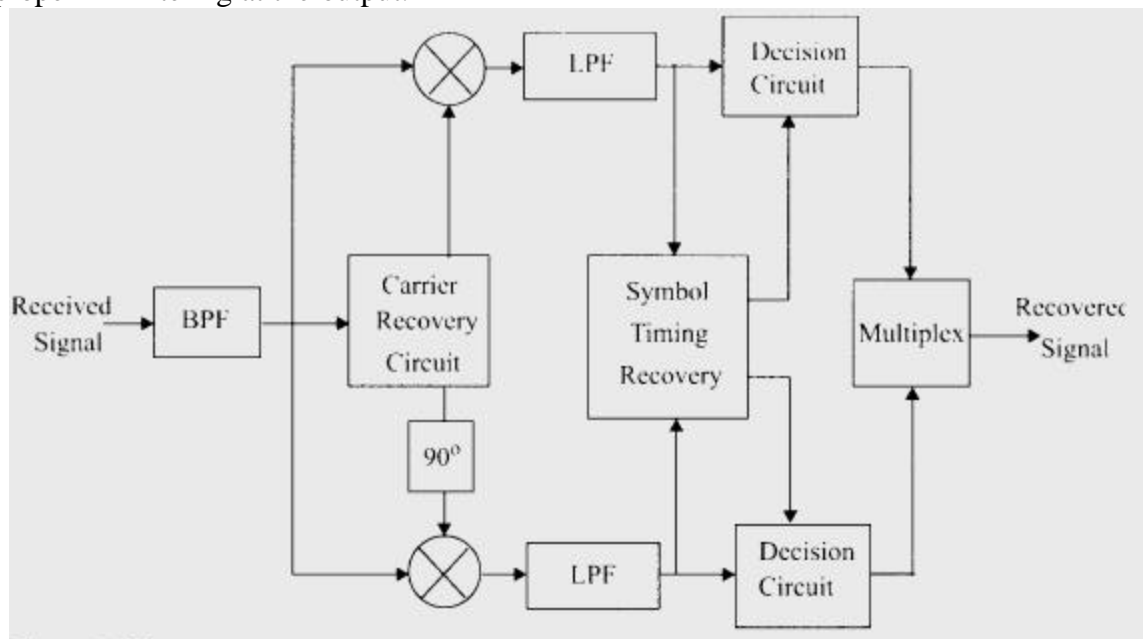
Null-to-null bandwidth is equal to the bit rate  $R_b$ , which is 1/2 of that of a BPSK signal as desired.



### QPSK Transmitter and Receivers:



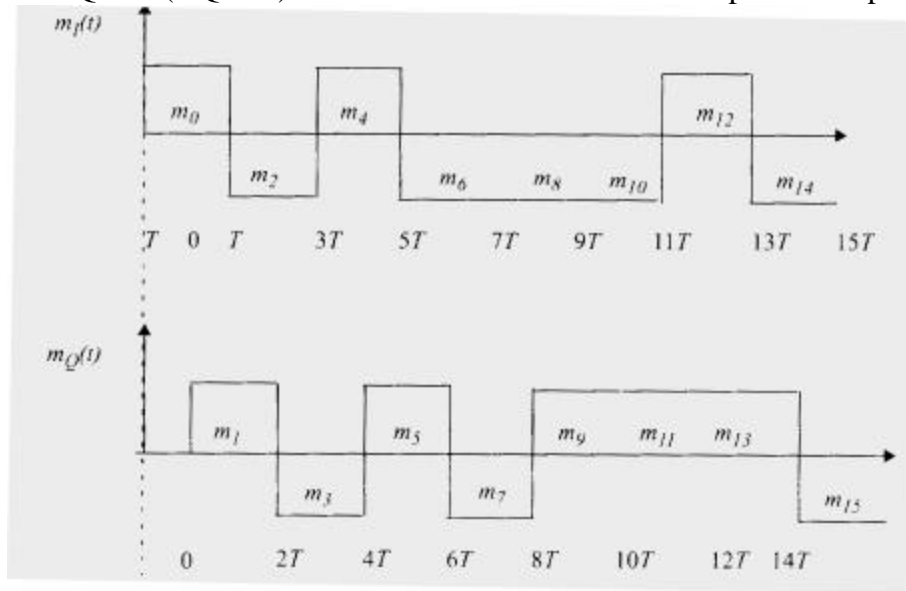
1. Unipolar binary messages are converted into bipolar NRZ sequence.
2. The bit stream is split into in-phase (even) and quadrature (odd) bit streams  $m_1(t); m_0(t)$  each with a bit rate  $R_s = R_b / 2$ .
3. Two orthogonal carriers separately modulate two binary sequences.
4. They are summed to produce a QPSK signal.
5. The bandpass filter at the output prevents the spillover of signal energy into adjacent channels and also removes the out-of-band spurious signals generated during the modulation process. In most wireless and other RF implementations, pulse shaping is done at the baseband to provide proper RF filtering at the output.



6. Front-end BPF removes the out-of-band noise and the interchannel interference and each part of the filter output is coherently demodulated.
7. The decision circuits very similar to BPSK systems process the outputs of demodulators.

- **Offset QPSK (OQPSK):**

This modified QPSK system is designed to combat the following ill of QPSK systems: The amplitude of a QPSK signal is ideally constant. However, they are normally pulse-shaped for efficiency and then they lose the constant envelope property. Occasional phase shift of  $\pi$  can cause the signal envelope to have a Z.C. Any kind of hard-limiting or non-linear amplification of the Z.C. brings back the filtered sidelobes since the fidelity of the signal at small voltage levels is lost in transmission. To prevent the regeneration of sidelobes and spectral spreading, it is imperative that only linear amplifiers, which are costly and very inefficient, are used for amplifying QPSK signals. If the in-phase and quadrature bit streams of QPSK signals are offset in their relative alignment by one-bit period (half-symbol rate), then this modified version of QPSK is called an Offset QPSK (OQPSK) and it results in more efficient amplification process.



1. Since the transition instants of  $m_I(t)$  and  $m_Q(t)$  are offset, at any given time only one bit stream can change values and maximum phase-shift is only  $\pm 90^\circ$ , which eliminates Z.C.
2. Obviously, there will be some ISI caused especially at the phase transition points. But the envelope variations are much less and non-linear amplifiers do not generate H.F. sidelobes.
3. Spectrum and BER of OQPSK are identical to those of QPSK and it is very attractive for wireless communications due to their improved performance even if there is phase jitter.

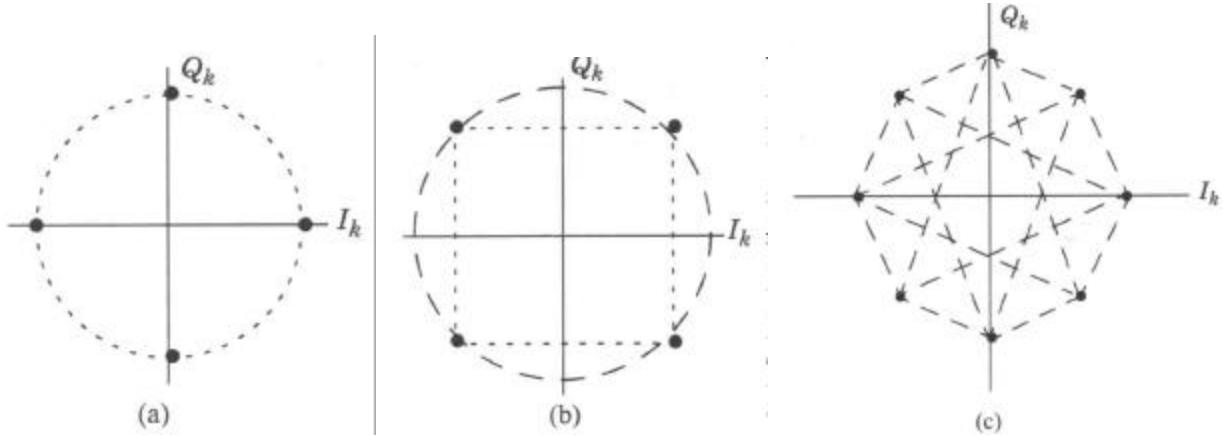
- **$\pi/4$ -QPSK**

$\pi/4$  Shifted QPSK offers a compromise between OQPSK and QPSK in terms of the allowed maximum phase transitions.

1. It may be demodulated in a coherent or non-coherent fashion.
2. Maximum phase change is limited to  $\pm 135^\circ$  and hence, it preserves the constant envelope property better than bandlimited QPSK.
3. It is more susceptible to envelope variations than OQPSK.
4. Non-coherent detection capability is an extremely attractive feature for simplifying receiver design.
5. In the presence of multipath spread and fading, it is observed to perform better than others do.



6. Very often they are differentially encoded to facilitate the implementation and they are called  $\pi/4$  DQPSK.
7. Constellations are depicted below.



Constellation diagram of a  $\pi/4$ -QPSK signal. (a) states for  $\mathbf{q}_k$  when  $\mathbf{q}_{k-1} = n\pi/4$ ; (b) when  $\mathbf{q}_{k-1} = n\pi/2$ ; (c) all possible states.

In-phase and quadrature pulses,  $I_k; Q_k$  over the time interval  $kT \leq t \leq (k+1)T$  are determined by their previous values as well as  $\mathbf{q}_k$ , which itself is a function of  $\mathbf{f}_k$ , which is a function of the current input symbols  $m_{Ik}, m_{Qk}$ . That is:

$$I_k = \text{Cos}(\mathbf{q}_k) = I_{k-1} \cdot \text{Cos}\mathbf{f}_k - Q_{k-1} \cdot \text{Sin}\mathbf{f}_k \quad (4.18)$$

$$Q_k = \text{Sin}(\mathbf{q}_k) = I_{k-1} \cdot \text{Sin}\mathbf{f}_k + Q_{k-1} \cdot \text{Cos}\mathbf{f}_k \quad (4.19)$$

$$\mathbf{q}_k = \mathbf{q}_{k-1} + \mathbf{f}_k \quad (4.20)$$

and the following table gives the phase shifts.

Information Bits $m_{Ik}$ and $m_{Qk}$	Phase Shift $\mathbf{f}_k$
1 1	$\pi/4$
0 1	$3\pi/4$
0 0	$-3\pi/4$
1 0	$-\pi/4$

The transmitter block diagram is shown below, where the in-phase and quadrature bit streams are separately modulated by two carriers which are in quadrature with one another and the  $\pi/4$ -QPSK waveform is given by:

$$S_{\pi/4\text{-QPSK}}(t) = I(t) \cdot \text{Cos}\omega_c t - Q(t) \cdot \text{Sin}\omega_c t \quad (4.21)$$

where:

$$I(t) = \sum_{k=0}^{N-1} I_k \cdot p(t - kT_s - T_s/2) = \sum_{k=0}^{N-1} \text{Cos}\mathbf{q}_k \cdot p(t - kT_s - T_s/2) \quad (4.22a)$$

$$Q(t) = \sum_{k=0}^{N-1} Q_k \cdot p(t - kT_s - T_s/2) = \sum_{k=0}^{N-1} \text{Sin}\mathbf{q}_k \cdot p(t - kT_s - T_s/2) \quad (4.22b)$$

Both  $I_k, Q_k$  are passed through Raised-Cosine roll-off pulse shaping filters before modulation to reduce the bandwidth occupancy.

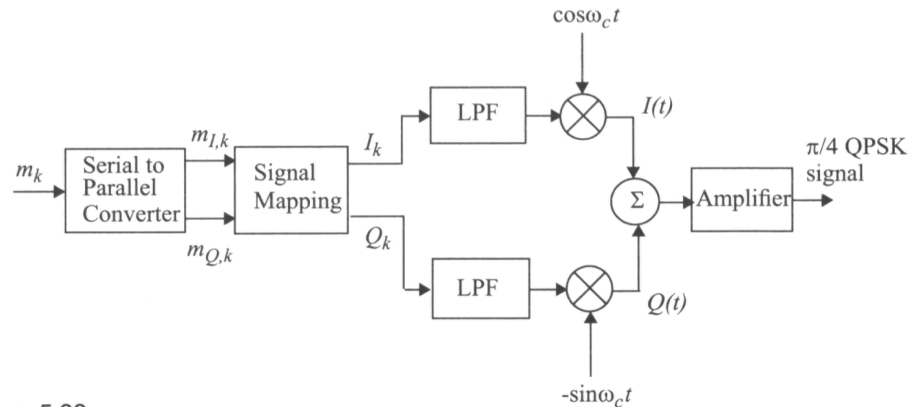


Figure 5.32  
Generic  $\pi/4$  QPSK transmitter.

- **Detection techniques for p/4 DQPSK:**

There are various types of detection techniques used for these signals, including "baseband differential detection, IF differential detection, and FM discriminator detection." Simulations show that all 3 receiver configurations offer similar BER, although there are implementation issues, which are specific to each technique. (Details of these are neatly presented in Rappaport [11]) and we will only present the block diagram of the baseband differential detector here.

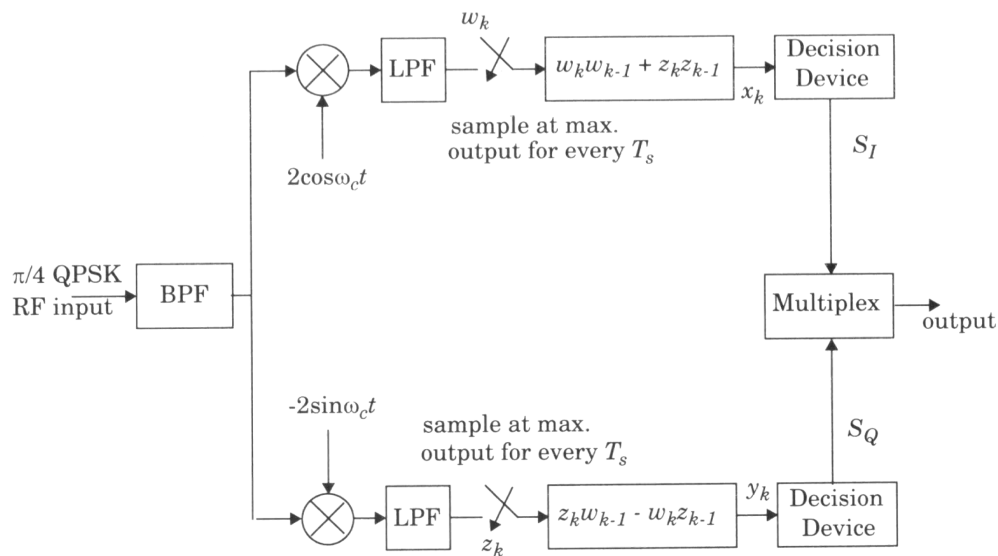


Figure 5.33  
Block diagram of a baseband differential detector [From [Feh91] © IEEE].

## 4.4 Quadrature Amplitude Modulation (QAM)

When the bandwidth efficiency is of primary importance and  $M$  is large, the constellation points on a circle become progressively less energy efficient and  $M$ -PSK signaling schemes are no longer of practical interest. If the channel exhibits good amplitude linearity, then  $M$ -level amplitude

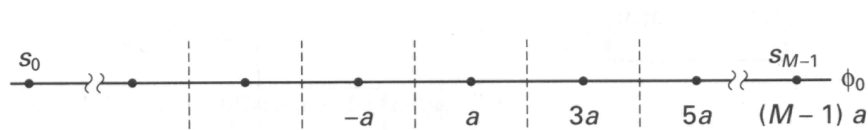
modulation (M-Am) and its extension to amplitude modulation of phase-quadrature carriers become more energy efficient. This last family of techniques is commonly known as QAM or M-ary AM/PM modulation and it has become irreplaceable in data communication over POTS.

- To derive the performance curves let us first consider the case of M-AM with M-even, where the transmitted signal is related to the data symbol  $m_i; i = 0, 1, \dots, M - 1$  through:

$$S_i(t) = (2m_i - M + 1)f(t) \quad (4.23)$$

and  $f(t)$  is a common signal shape to all signals, either a baseband pulse or a burst of a carrier frequency signal; such as Raised-Cosine Filtered pulse.

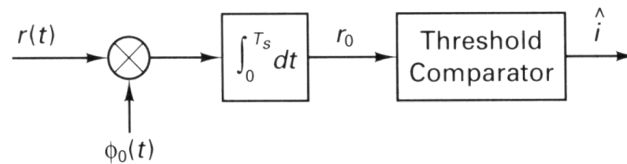
- The signal constellation in 1-D for this signal set is equally spaced points as shown below.



- Average energy associated with this set is obtained by summing the squares of odd integers and averaging:

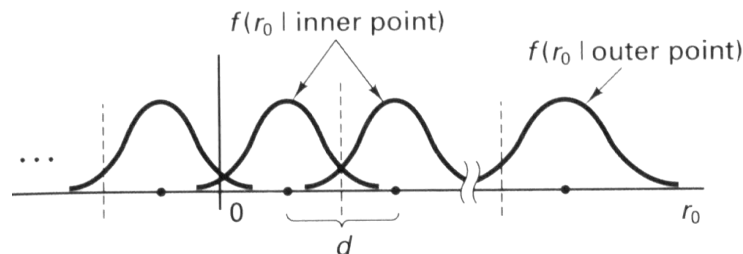
$$E_s = (M^2 - 1)a^2 / 3 \quad (4.24)$$

- The optimum receiver in basis function form, where we generate a scalar statistic and compare with a set of thresholds  $0, \pm a, \pm 2a, \dots$ , the basic M-AM receiver is similar to that of a QAM as shown below:



### Probability of Error for M-AM

Consider the conditional pdf plots of inner and outer points as shown in the following picture.



The symbol error probability is:

$$P_s(\mathbf{e}) = \frac{M-2}{M} \cdot P(\mathbf{e} | \text{inner point}) + \frac{2}{M} \cdot P(\mathbf{e} | \text{outer point}) \quad (4.25)$$

It has been shown in literature that this has a close form:

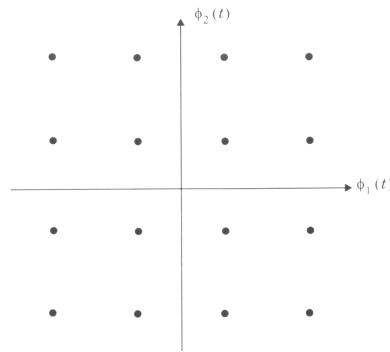
$$P_s(\mathbf{e}) = \frac{2(M-1)}{M} \cdot Q\left(\sqrt{\frac{6E_b \cdot \log_2 M}{N_0(M^2-1)}}\right) \quad (4.26)$$

To minimize the bit error probability, Gray coding of the amplitude levels are used and then BER can be approximated for large M by:

$$BER = P_b(\mathbf{e}) \approx \frac{2}{\log_2 M} \cdot Q\left(\sqrt{\frac{6E_b \cdot \log_2 M}{N_0(M^2-1)}}\right) \quad (4.27)$$

### M-ary QAM:

Now let us modulate the previous case, as in the QPSK, by  $\text{Cos}w_c t$  and  $\text{Sin}w_c t$  to obtain in-phase and quadrature components of M-AM signals as shown in constellations below.



General form of an M-ary QAM signal can be defined as:

$$S_i(t) = \sqrt{\frac{2E_{\min}}{T_s}} \cdot [a_i \cdot \text{Cos}(w_c t) + b_i \cdot \text{Sin}(w_c t)] \quad (4.28)$$

for  $0 \leq t \leq T_s$  and  $i = 1, 2, \dots, M$  and where  $E_{\min}$  is the energy of the signal with the lowest amplitude.  $\{a_i, b_i\}$  are pair of independent integers chosen according to the location of a particular signal point. If rectangular pulse shapes are used then the signal is expanded in terms of two basis functions:

$$f_1(t) = \sqrt{\frac{2}{T_s}} \text{Cos}(w_c t) \quad (4.29a)$$

and

$$f_2(t) = \sqrt{\frac{2}{T_s}} \text{Sin}(w_c t) \text{ in } 0 \leq t \leq T_s \quad (4.29b)$$

The coordinates of the  $i^{\text{th}}$  message points are  $\{a_i \sqrt{E_{\min}}, b_i \sqrt{E_{\min}}\}$ , where  $\mathbf{L} \times \mathbf{L}$  matrix gives:

$$\{a_i, b_i\} = \begin{bmatrix} (-L+1, L-1) & (-L+3, L-1) & \dots & (L-1, L-1) \\ (-L+1, L-3) & (-L+3, L-3) & \dots & (L-1, L-3) \\ \vdots & \vdots & \vdots & \vdots \\ (-L+1, -L+1) & (-L+3, -L+1) & \dots & (L-1, -L+1) \end{bmatrix} \quad (4.30)$$

Note that  $L = \sqrt{M}$ .

- For this type of signaling, the probability of error with coherent detection has been found to be approximately:

$$P_{QAM}(\mathbf{e}) \cong 4\left(1 - \frac{1}{M}\right) \cdot Q\left(\sqrt{2E_{\min} / N_0}\right) \tag{4.31}$$

- In terms of average signal energy this can be expressed as:

$$P_{QAM}(\mathbf{e}) \cong 4\left(1 - \frac{1}{M}\right) \cdot Q\left(\sqrt{3E_{av} / (M - 1)N_0}\right) \tag{4.32}$$

- More critically than this last expression would be a performance formula in terms of an efficiency factor, normalized to the case of "antipodal or BPSK signaling." An upper bound for the probability of error in this fashion has been found to be:

$$P_{QAM}(\mathbf{e}) \leq 4 \cdot Q\left(\frac{d}{\sqrt{2N_0}}\right) \cong 4 \cdot Q\left(\sqrt{\frac{2E_b}{N_0} h_M}\right) \tag{4.33}$$

**Note 1:** PSD and bandwidth efficiency of QAM is identical to M-ary PSK modulation.

**Note 2:** Relative Power or energy efficiencies of M-AM and M-QAM with respect to antipodal design are given in the following table.

$M_{AM}$	$M_{QAM}$	$\eta_M$ , dB
4	16	-4.0
-	32	-6.0
8	64	-8.5
-	128	-10.2
16	256	-13.3

**Figure 3.3.26** Relative energy efficiencies for M-AM and M-QAM normalization is to antipodal design

**Example 4.1:** Find the Error Probability for 32-point QAM

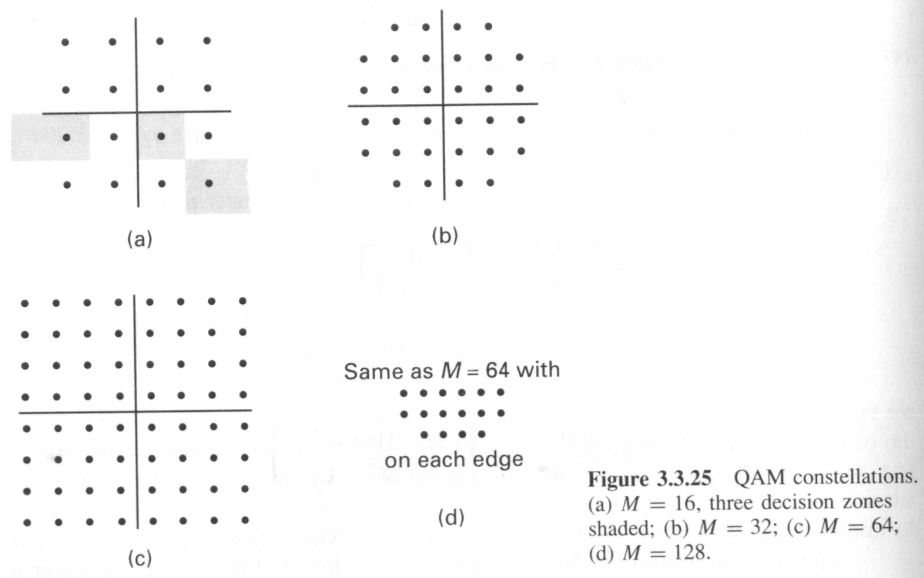


**Figure 3.3.25** QAM constellations. (a)  $M = 16$ , three decision zones shaded; (b)  $M = 32$ ; (c)  $M = 64$ ; (d)  $M = 128$ .

- 32-point QAM constellation in the figure below is scaled to have signal spacing:  $d = 2a$  in each dimension.
- Different energy numbers are:  $2a^2, 10a^2, 18a^2, 26a^2, 34a^2$
- Populations at these energies are: 4, 8, 4, 8, 8
- Assume equiprobable selection of all messages then average Energy using the energy values and populations above:

$$E_{av} = E_s = 20a^2 = 5d^2 \Rightarrow d = \sqrt{E_s/5}$$

- Using  $E_s/N_0 = 5E_b/N_0$  in the probability of error expression we obtain:

$$P_{32-QAM}(\mathbf{e}) \leq 4 \cdot Q\left(\sqrt{\frac{2E_b}{N_0} \cdot \frac{1}{4}}\right) \quad (4.34)$$

This result indicates a relative efficiency of  $10 \cdot \log(1/4) = -6.0 \text{ dB}$  over BPSK.

**Note 1:** For 2-D QAM we may quadruple M in exchange for increasing SNR:  $E_b/N_0$  by 6.0 dB as shown in the above tabulation. This increases dimensional efficiency by 2-bits/2-Dim.

**Note 2:** According to the previous comment that QAM offers no intrinsic benefit over M-AM. But the QAM format really does gain by a factor of 2 in spectral (BW) efficiency for the same energy efficiency, extending the superiority of QAM over QPSK.

**Note 3:** To minimize BER, proper bit labeling should be made to ensure that adjacent signal points differ in as few bits as possible, such as the Gray-coded bit assignment for square constellations.

#### 4.5 Multi-Dimensional Lattice Based Constellations

Fundamental problem in digital communication formats is to locate M signal points in a one- or two- or higher-dimensional space so that the minimum intra-signal distance is some target value  $d$ , and so that the average energy (or alternatively, the peak energy) of the constellation is minimized.

- For 1-D signal constellations, the solution is the trivial case of placing points equally spaced along the real-line symmetrically about the origin.
- In 2-D, placing points on the 2-D grid offers no intrinsic gain in packing efficiency over 1-D arrangement. But there is a more dense regular arrangement of two-dimensional points.

**Example 4.2:** Arrange coins on the table with a hexagonal sphere-packing. (I.e. place centers of coins at the vertices of an equilateral triangle.). In this case, the nearest-neighbor decision zone -- commonly known as the Voronoi Region in the VQ jargon-- is proven to be 15% more dense than the 2-D grid, or rectangular packing we have used above. This 15% gain reflects as 0.6 dB increase in the energy efficiency for the optimal packing.

- A systematic means of describing large sets of points in N-dimensional Euclidean space involves **Lattices**. There are a number of good lattices that could be utilized for AM/QAM designs. Examples of 3-D lattice structures are shown below.

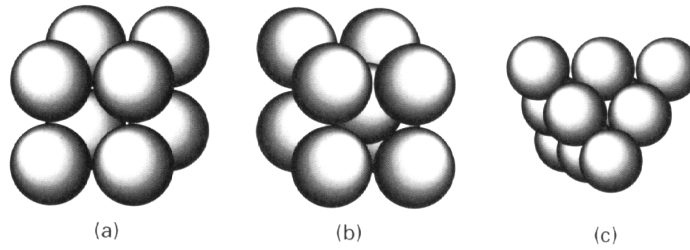
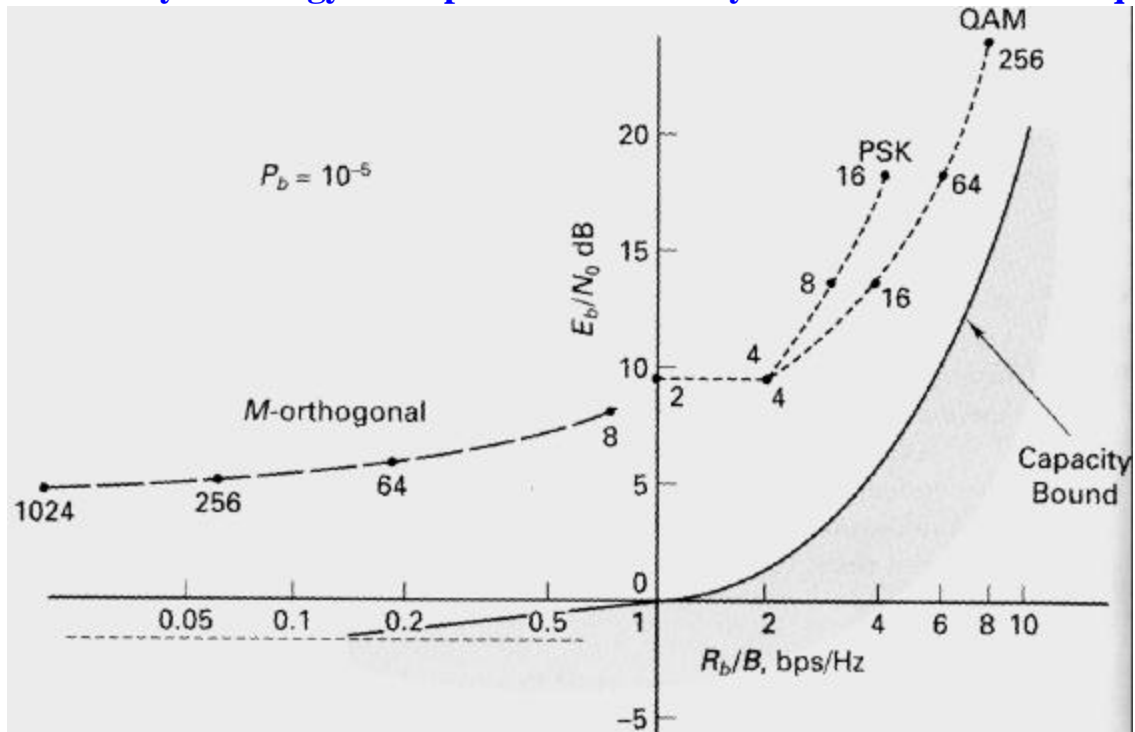


Figure 3.3.28 Three-dimensional sphere packings. (a) Simple cubical packing; (b) body-centered cubical packing; (c) face-centered cubical packing.

- There is a fairly comprehensive coverage of this material in Wilson (18) and readers are recommended to refer to pages of that reference (196-201).

#### 4.6 Summary of Energy and Spectrum Efficiency of Modulation Techniques



1. For the M-ary signaling within the PSK/QAM/PAM class, let the bit rate be  $R_b$  b/s, the symbol rate is simply  $R_s = R_b / \log_2 M$  symbols-per-second (sps), and the bandwidth can theoretically be as small as:

$$B = R_b / \log_2 M \text{ Hz.} \quad (4.35)$$

2. We can define the spectral (bandwidth) efficiency as:

$$\mathbf{h}_B \equiv \frac{R_b}{B} = \frac{2 \log_2 M}{M} \text{ bps / Hz} \quad (4.36)$$

3. A factor of 2 increase in spectral efficiency is possible for bi-orthogonal signaling since the number of dimensions occupied by the signal constellation is only  $MR_b/2$ .
4. Plots above span a large range of energy/bandwidth efficiencies, but comparing typical modulations with the capacity bound for the bandlimited AWGN channel, it is reasonable to assert that the potential saving in  $E_b/N_0$  is within 9 dB, while maintaining the same spectral efficiency.

**Note:** Trellis-Coded Modulation (TC), Discrete Multi-tone Modulation (DTM), and the Carrierless Amplitude Modulation (CAP) techniques will be covered later in this workshop.